LETTERS

Neutron and X-ray diffraction study of the broken symmetry phase transition in solid deuterium

Igor Goncharenko[1] & Paul Loubeyre[2]

The solid hydrogen compounds D_2, HD and H_2 remain quantum molecular solids up to pressures in the 100 GPa range[1]. A remarkable macroscopic consequence is the existence of a pressure-induced broken symmetry phase transition[2–4], in which the molecules go from a spherical rotational state to an anisotropic rotational state. Theoretical understanding of the broken symmetry phase structure remains controversial, despite numerous studies[5–10]. Some open questions concern the existence of long- or short-range orientational order; whether a strong isotopic shift on the transition pressure should be assigned to the nuclear zero-point motion or to quantum localization; and whether the structures are cubic, hexagonal or orthorhombic. Here we present experimental data on the structure of the broken symmetry phase in solid D_2, obtained by a combination of neutron and X-ray diffraction up to 60 GPa. Our data are incompatible with orthorhombic structures predicted by recent theoretical works. We find that the broken symmetry phase structure is incommensurate with local orientational order, being similar to that found in metastable cubic *para*-D_2.

In the ground state at low temperature and low pressure, hydrogen molecules are in the $J = 0$ spherical rotational states[11]. When pressure is applied, the molecules are driven closer to each other, so that at high enough pressure the new equilibrium state of the system is given by a trade-off between going higher in kinetic energy (that is, to $J \neq 0$ rotational levels) and gaining a negative potential energy through a orientational ordering that minimizes electric quadrupole–quadrupole (EQQ) energy. First-principles calculations show[6,12] that the EQQ interactions dominate over other interactions in the pressure range up to 100 GPa. Surprisingly, the increase in ordering by the admixture of the $J \neq 0$ states is not gradual. A first-order phase transition from the orientationally disordered phase to the orientationally ordered phase was first predicted[13] in *para*-H_2 and *ortho*-D_2 at a pressure of ~15–30 GPa, accompanied by a structural transition from hexagonal close packed (h.c.p.) to face-centred cubic (f.c.c.). It was then observed that the broken symmetry phase (BSP) transition in fact occurs with a strong isotopic shift in the transition pressure, respectively 28 GPa for D_2 (ref. 2), 69 GPa for HD (ref. 4) and 110 GPa for H_2 (ref. 3). The orientationally disordered and ordered phases were also named as phase I and phase II, respectively. Furthermore, detailed spectroscopic studies have shown that the persistence of the optical phonon in phase II should imply that the h.c.p. structure of the molecular centres is not strongly affected by the orientational order[14].

The calculation of the structure of the BSP poses a complex many-body problem, because it must embody the quantum character of the nuclei. A large number of calculations, based on different approximations, have tackled this problem, with some controversy. The first-principles calculations based on density functional theory (DFT) suggest $Cmc2_1$ (ref. 6), $Pca2_1$ (refs 7, 9, 10) or $P2_1/c$ (ref. 8) structures in phase II. In these structures, the molecular centres do not deviate significantly from the h.c.p. lattice, but the molecules are ordered in the *a*–*b* plane with a polar angle in the range 40–70°. All the above structures are orthorhombic, with four molecules per unit cell. Another approach is to use realistic interactions between the molecules, and to solve quasi-exactly the hamiltonian of the interacting nuclei by a path integral Monte Carlo simulation[5,15]. One such calculation[5] suggests a *Pa*3-type local orientation of the molecules and without displacement of their molecular centres from the h.c.p. lattice. No long-range structure was proposed in this work. Finally, it should be noted that the structure of phase II is an interesting solution of the model of coupled quantum rotors, which has been applied to various physical systems[15].

The only direct experimental methods available to study crystal structure in the high-pressure phases of H_2 and D_2 are X-ray or neutron scattering experiments. D_2 or H_2 have no inner electronic shells, and X-rays are scattered by electrons in molecular orbitals. Therefore X-rays are almost insensitive to individual positions of H(D) atoms in the molecules and to orientational ordering. Contrarily, neutrons are scattered by individual nuclei, and therefore can be used to determine the individual positions of H(D) in the structure, as well as the orientations of the molecules. Because of the very small scattering power of a hydrogen crystal in a diamond anvil cell, the use of a third-generation synchrotron source and the growth of a single crystal in helium were previously needed to measure the equation of state of H_2 and D_2 to 120 GPa at 300 K (ref. 16). This X-ray approach has been extended here to low temperature. Owing to the low intensity of neutron sources, the high-pressure neutron study of the hydrogens is more challenging. Recent progress in pressure techniques and neutron instrumentation at the Laboratoire Léon Brillouin[17] is used here to push the pressure limits for single-crystal neutron diffraction experiments. We present below a combination of neutron and X-ray techniques (up to 38 GPa and 60 GPa respectively, down to 1.5 K) to solve the structure of phase II.

Four different D_2 crystals were studied by X-ray diffraction: two of them were embedded in helium pressure transmitting medium. In one run, the single crystal of D_2 in helium was cooled at a constant pressure of 63.4 GPa and the (100), (101) and (002) reflections were measured. As seen in Fig. 1a, a small positive discontinuity in the lattice parameter c ($\Delta c/c = 3 \times 10^{-4}$) was observed at 70 K. A negative discontinuity in the parameter a ($\Delta a/a = -6 \times 10^{-4}$) was also observed at 70 K. This gives a transition point to phase II that is in excellent agreement with previous spectroscopic studies, and the corresponding volume discontinuity, $\Delta V/V = -10^{-3}$, confirms a previous estimate from the Clapeyron equation and the slope of the I–II boundary line[1,18]. We note that the orthorhombic structures with the polar angle of the molecule almost in the *a*–*b* plane should give a negative discontinuity in c of about 1% (ref. 7), whereas a positive discontinuity is observed here. Two other runs have followed the evolution of reflections of the [100] and [101] class by going up in pressure at 25 K. One crystal had helium as pressure transmitting medium and the other did not. As seen in Fig. 1b, no discontinuity of the 100 *d*-spacing could be detected within the accuracy of the measurement. From X-ray measurements, we find that the I–II transition does not affect the diffraction peaks of the h.c.p. lattice, except for a very small volume discontinuity. Yet, as seen below, a transition was observed in both cases at around 16 GPa, as determined from the appearance of a superstructural peak.

One single crystal of D_2 in helium was devoted to the neutron measurements. The mosaicity and the orientation matrix of the single crystal were first determined by X-ray diffraction. The neutron data were collected at 38 GPa in the temperature range 1.5–70 K, above and below the I–II transition (I–II transition temperature $T_{I\text{-}II} \simeq 44$ K at 38 GPa). The (100), (010), (110), (101), (110), (110) and (002) reflections were collected. As seen in Fig. 2, the quality of the crystal (rocking curve of 1°) allows an accurate determination of the intensity of the various reflections (apart from the (002) reflection, which was contaminated by a diamond reflection). In Fig. 2, integrated intensities of various neutron reflections are plotted versus temperature and compared to the expected behaviour of the strongest candidates for the structure of phase II. Surprisingly, none is satisfactory. All being of an orthorhombic symmetry, they give non-equivalent intensities for (100), (010) and (110) reflections (all indices are given in the hexagonal unit cell), whereas exactly the same intensity is observed (see inset in Fig. 2b). We could then assume that the orthorhombic symmetry is shadowed by twinning along the crystallographic directions linked by the *P*3 symmetry of phase I. The sample would then consist of three equivalently populated orthorhombic domains, with *a* axes directed along the [100], [010] or [110] directions of the unit cell of phase I. Even under this assumption, the predicted intensities from $Cmca$ and $Cmc2_1$ structures completely disagree with the experimental data. $P2_1/c$ and $Pca2_1$ structures explain the intensity of the (101) reflection, but not that of the (100) and (110) reflections. Assuming any non-equivalent domain distribution would only increase the difference between experiment and the predicted structures.

To explain the data, we follow the theoretical prediction[5] that the I–II transition is purely rotational with a *Pa*3-type local order. The *Pa*3 structure is the structure observed in pure *ortho*-D_2 or *para*-H_2 (metastable in the $J = 1$ rotational state), which orders at low temperature in a cubic close-packed structure with neighbouring molecules directed along the different cubic diagonals[11]. This structure minimizes the EQQ energy for a three-dimensional compact structure. To transpose a similar type of order on a hexagonal lattice, the molecules form four sublattices with molecular axes directed perpendicular to the four different faces of a tetrahedron. The

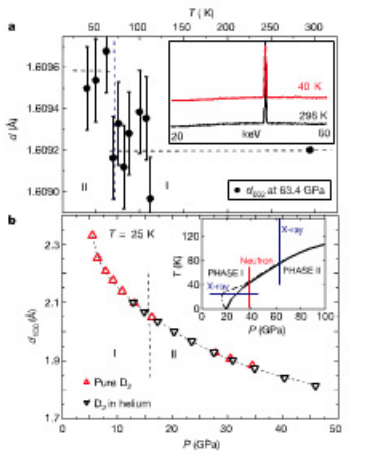

Figure 1 | X-ray diffraction measurements at the I–II phase transition in solid D_2. **a**, Evolution with temperature (T) of the *d*-spacing at 63.4 GPa, as measured by EDX. Filled circles are data points; error bars correspond to the 2×10^{-4} precision of the EDX measurement. The inset shows the (002) peak measured in phase I at 296 K (black) and in phase II at 40 K (red). **b**, Evolution with pressure (P) of the *d*-spacing of the (100) reflections measured by ADX at 25 K. The black and red triangles indicate data from a single crystal of D_2 respectively with and without helium pressure transmitting medium. The inset shows the pressure–temperature domains of the X-ray (in blue) and neutron (in red) measurements in the phase diagram. The solid and dashed black lines show respectively the I–II boundary line as determined from spectroscopic data[1,18] and the re-entrant behaviour proposed here.

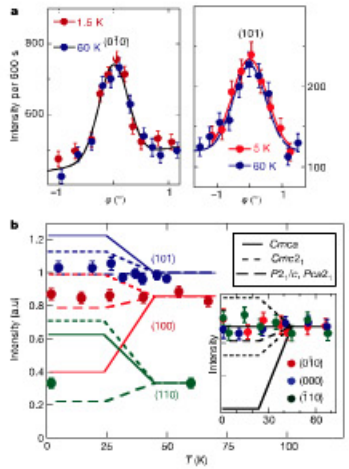

Figure 2 | Neutron diffraction measurements at the I–II phase transition on a single crystal of D_2 at 38 GPa with helium pressure transmitting medium. Error bars are statistical errors (data are shown as mean ± standard deviation) in the neutron experiment. Other contributions to the errors are negligible compared to the statistical error. **a**, Neutron intensities of the (010) and (101) reflections versus rocking angle ϕ in phase I (blue) and phase II (red). **b**, Comparison between experiment and the predicted neutron intensity for various structures. The predicted intensities have been averaged over the reflections linked by the *P*3 symmetry assuming an equivalent domain distribution of twin crystals. Also, the atomic displacements $\langle U^2 \rangle$ given in ref. 6 (scaled to a pressure of 38 GPa and for the mass of a deuteron) were included in the calculation. Filled circles, experiments; horizontal lines, calculated intensities for different orthorhombic models; sloping lines, guides for the eye. Inset, calculation for a single domain crystal of the (100), (010) and (110) reflections linked by *P*3 symmetry.

[1]Laboratoire Léon Brillouin CEA-CNRS, CEA Saclay, 91191 Gif-sur-Yvette, France. [2]Département Physique Théorique et Applications, CEA, 91680 Bruyères-le-Châtel, France.

molecules are then arranged so that every molecule is surrounded by molecules belonging to the other three sublattices. A schematic drawing of the structure is shown in Fig. 3a (projection in the *a*–*b* plane). The unit cell is of $P\bar{3}$ symmetry, and consists of eight molecules. The neutron intensities calculated with this structure are seen in Fig. 3c to be in good agreement with the experimental data.

The *Pa*3-type of local order has a topological frustration when built in a hexagonal lattice. Whereas in the cubic structure the four sublattices correspond to four high-symmetry directions, in the h.c.p. structure the four orientations should be chosen from seven possible directions in the '5 × D_3' bipyramid (perpendicular to three 'up' and three 'down' faces and one along the *c* axis; Fig. 3b). There are no physical reasons to choose between 'up' and 'down' directions. An attempt to avoid the frustration by fixing the molecular axis in the *a*–*b* plane leads to the $P6_3/m$ structure previously proposed[19,20] for $J = 1$ hydrogen. But, as shown in Fig. 3c, this model does not satisfy the neutron data. Stacking faults between the 'up' and 'down' configurations should develop. If randomly distributed, they should give a short-range ordered structure. If collectively arranged, they should give an incommensurate long-range order. As shown in Fig. 4, incommensurate reflections with X-rays and with neutrons are indeed observed in phase II. The incommensurate vector is lying along the (100) direction. When the D_2 single crystal is embedded in helium, the incommensurate peak is observed along only one of the [100] directions, whereas when no pressure transmitting medium is used incommensurate peaks are observed along all three {100}, {010} and {110} directions, because of twinning of the crystal under non-hydrostatic stress. No superstructure was observed along the *c* direction.

As seen in Fig. 4, the incommensurate peak appears reproducibly at the BSP transition, and is in fact the strongest structural signature of the phase transition. The transition is observed at 16 GPa at 25 K, whereas it has been measured between 20 GPa (ref. 14) and 24 GPa (ref. 18) at 5 K. This could be explained as follows: whereas at $T < 5$ K the equilibrium concentration of *para*-D_2 is practically zero (<0.1%), at 25 K it increases to ~5%. The $J = 1$ states favour the BSP transition occurring at lower pressure, resulting in a re-entrant shape of the I–II boundary line (see Fig. 1b inset). The re-entrant behaviour has been clearly observed for HD (ref. 4) and was predicted for D_2 with equilibrium *ortho*–*para* concentration[21]. The incommensurate vector measured at 25 K by X-ray diffraction is essentially the same as the incommensurate vector measured by neutron diffraction at 1.5 K after the sample was kept for several days at this temperature in order to complete *para*–*ortho* conversion. Furthermore, we observed no changes in neutron intensities of the structural peaks measured at 38 GPa between 25 K and 1.5 K and over a few days of equilibrium time. Hence, we believe that at 38 GPa the modest $J = 1$ concentrations have no drastic effect on the type of orientational ordering. The structure described above should be representative for pure *ortho*-deuterium. But additional measurements are required to investigate the influence of $J = 1$ states on specific regions of the pressure–temperature phase diagram, especially near the onset of the BSP transition.

The purely orientational transition on the h.c.p. lattice with *Pa*3-type local order seems to fit the structural data presented here. It also gives an explanation (involving frustration) of the incommensurate modulation of the structure. Also, the incommensurate modulation lowers the symmetry of the h.c.p. lattice, and hence could explain the multiplet structure of the roton bands and the additional vibron bands in the Raman and infrared spectra of phase II (ref. 14). Yet it remains to be understood why the *d*-spacing of the incommensurate peak is rather close to that of the (002) structural reflection. We note that the *Pa*3-type local order and incommensurate structures were not considered in DFT simulations. This should motivate further theoretical work. Finally, similar structural studies could be extended to higher pressures to characterize phase II of the other hydrogen isotopes, HD and H_2. It could be that the structure of phase II depends on the isotope[22].

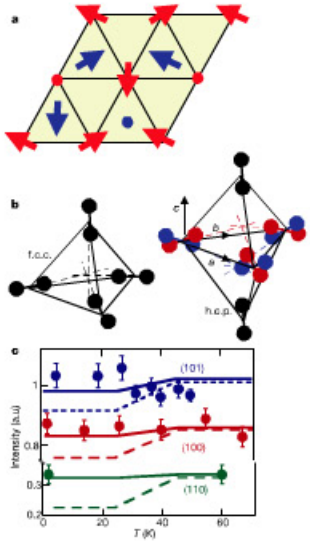

Figure 3 | Proposed structure for phase II of D_2. **a**, Projection of the $P\bar{3}$ local structure to the *a*–*b* plane. Red and blue colours indicate molecules centred in the planes $z = 0$ and $z = 0.5$, respectively. Arrows point to the positive *z*-hemisphere, circles depict molecules lying along the *c*-axis. **b**, Left, orientational order in the f.c.c. lattice (*Pa*3 structure). Molecular axes are directed towards the centre of the tetrahedron. Right, frustration in the h.c.p. lattice. In red and blue we show two different orientations (towards the centres of the upper and lower tetrahedrons, respectively) that have the same EQQ energy. Alternating 'red' and 'blue' configurations result in a superstructure in the (*a*–*b*) plane. **c**, Calculated intensities for the $P\bar{3}$ (full lines) and $P6_3/m$ (dashed lines) structures versus experimental data (filled circles). Error bars are statistical errors (data are shown as mean ± standard deviation). Sloping lines are guides for the eye.

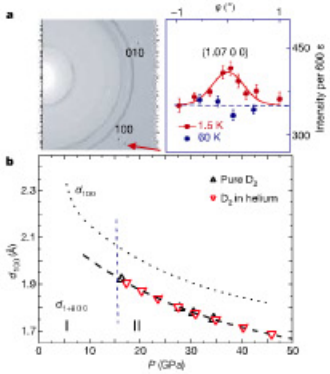

Figure 4 | Experimental evidence of a superstructure in phase II. **a**, Left, (100) and (010) reflections of a single crystal of D_2 in helium at 40 GPa. The diffraction peaks were recorded on an image plate detector during an oscillation of the diamond anvil cell (−20° to 20°) in the ADX configuration. The arrow indicates the (1.07 0 0) incommensurate peak. No incommensurate reflection is observed along the (010) reflection. The continuous diffraction rings are from the pressure cell. Right, neutron rocking curve of the incommensurate (1.07 0 0) reflection measured at 38 GPa. The incommensurate reflection reversibly disappears in phase I. The red and blue data points indicate respectively measurements in phase II and phase I. Error bars are statistical errors (data are shown as mean ± standard deviation). **b**, Evolution of *d*-spacing of the (1+δ 0 0) peak versus pressure at 25 K. In D_2 with no pressure transmitting medium (black triangles), or D_2 in helium (red triangles), the incommensurate peak appears above 16 GPa.

METHODS

A new hybrid diamond anvil cell has been developed to perform both X-ray (large axial X-ray opening) and neutron (large radial neutron opening) diffraction and to allow H_2/He gas loading. The X-ray measurements were performed by energy dispersive X-ray (EDX; 1 run) and angular dispersive X-ray (ADX; 3 runs) techniques at the ESRF (ID09 and ID 30 beamlines). The (002) reflection was accessible in the EDX run only. The neutron diffraction experiments were performed on diffractometer 6T2 at the Laboratoire Léon Brillouin. Pressure was measured by using standard ruby fluorescence techniques corrected for low temperatures. The *ortho*–*para* conversion rate is expected to increase under very high pressures[14]. The conversion rate under pressure has been measured for hydrogen[15,16], but no quantitative measurements for solid deuterium have been performed so far. The samples were allowed 12–72 h to convert to an equilibrium *ortho*–*para* ratio. This procedure is consistent with the earlier spectroscopic works[17].

Received 21 January; accepted 28 April 2005.

1. Mazin, I., Hemley, R., Goncharov, A., Hanfland, M. & Mao, H. K. Quantum and classical orientational ordering in solid hydrogen. *Phys. Rev. Lett.* **78**, 1066–1069 (1997).
2. Silvera, I. F. & Wijngaarden, R. J. New low-temperature phase of molecular deuterium at ultrahigh pressure. *Phys. Rev. Lett.* **47**, 39–42 (1981).
3. Lorenzana, H. E., Silvera, I. F. & Goettel, K. A. Evidence for a structural phase transition in solid hydrogen at megabar pressures. *Phys. Rev. Lett.* **63**, 2080–2083 (1989).
4. Mashiary, F., Chen, N. & Silvera, I. Remarkable high pressure phase line and orientational order in solid hydrogen deuteride. *Phys. Rev. Lett.* **71**, 3814–3817 (1993).
5. Cui, T., Cheng, E., Alder, B. J. & Whaley, K. B. Rotational ordering in solid deuterium and hydrogen: A path integral Monte Carlo study. *Phys. Rev. B* **55**, 12253–12266 (1997).
6. Kitamura, H., Tsuneyuki, Sh., Tadashi, O. & Miyake, T. Quantum distribution of protons in solid molecular hydrogen at megabar pressures. *Nature* **404**, 259–262 (2000).
7. Kohanoff, J., Scandolo, S., Chiarotti, G. L. & Tosatti, E. Solid molecular hydrogen: The broken symmetry phase. *Phys. Rev. Lett.* **78**, 2783–2786 (1997).
8. Johnson, K. A. & Ashcroft, N. W. Structure and bandgap closure in dense hydrogen. *Nature* **403**, 632–635 (2000).
9. Stadele, M. & Martin, R. Metallization of molecular hydrogen: prediction from exact-exchange calculations. *Phys. Rev. Lett.* **84**, 6070–6073 (2000).
10. Nagao, K., Takezawa, T. & Nagara, H. Ab initio calculation of optical-mode frequencies in compressed solid hydrogen. *Phys. Rev. B* **59**, 13741–13753 (1999).
11. Van Kranendonk, J. Solid hydrogen: theory of the properties of solid H_2, HD, D_2 (Plenum, New York, 1983).
12. Kaxiras, E. & Guo, Z. Orientational order in dense molecular hydrogen: A first-principles path-integral Monte Carlo calculation. *Phys. Rev. B* **49**, 11822–11832 (1994).
13. Raich, J. & Etters, R. Rotational molecular motion in solid H_2 and D_2 under pressure. *J. Low Temp. Phys.* **6**, 229–240 (1972).
14. Goncharov, A. F., Eggert, J. H., Mazin, I. I., Hemley, R. J. & Mao, H. K. Raman excitations and orientational ordering in deuterium at high pressure. *Phys. Rev. B* **54**, R15590–R15593 (1996).
15. Freiman, Y., Tretyak, S., Antsygina, T. & Hemley, R. Novel phase behavior in quantum rotors. *J. Low Temp. Phys.* **133**, 251–260 (2003).
16. Loubeyre, P. *et al.* X-ray diffraction and equation of state of hydrogen at megabar pressures. *Nature* **383**, 702–704 (1996).
17. Goncharenko, I. N. Neutron diffraction experiments in diamond and sapphire pressure cells. *High Press. Res.* **24**, 193–204 (2004).
18. Cui, L., Chen, H., Leon, S. & Silvera, I. Megabar pressure triple point in solid deuterium. *Phys. Rev. Lett.* **72**, 3048–3051 (1994).
19. Miyagi, H. & Nakamura, T. Ground state energy difference of hcp and fcc ortho-hydrogens. *Prog. Theor. Phys.* **37**, 641–660 (1967).
20. James, H. Orientational order in solid ortho-hydrogen. Hexagonal close-packed molecular lattice. *Phys. Rev.* **167**, 862–874 (1968).
21. Helényi, B., Scandolo, S. & Tosatti, E. Theoretical evidence for a reentrant phase diagram in ortho-para mixtures of solid H_2 at high pressure. *Phys. Rev. Lett.* **94**, 125503 (2005).
22. Goncharov, A., Hemley, R., Mao, H. K. & Shu, J. New high-pressure excitations in parahydrogen. *Phys. Rev. Lett.* **80**, 101–104 (1998).
23. Pravica, M. & Silvera, I. F. NMR study of ortho-para conversion at high pressure in hydrogen. *Phys. Rev. Lett.* **81**, 4180–4183 (1998).
24. Eggert, J., Karmon, E., Hemley, R., Mao, H. K. & Goncharov, A. Pressure-enhanced ortho-para conversion in solid hydrogen up to 58 GPa. *Proc. Natl Acad. Sci. USA* **96**, 12269–12272 (1999).

Acknowledgements We thank A. Goukasov and O. Makarova for help in neutron experiments, and R. LeToullec, F. Occelli, M. Hanfland and M. Mezouar for help with the X-ray work.